Energy Proceedings
Vol 59, 2025
ISSN 2004-2965

Dynamic characteristics and influencing factors of CO_2 displacement in tight oil reservoirs assisted by direct current electric field#

Wenting Guo[1], Zhengfu Ning [1*]

1. School of Petroleum Engineering, China University of Petroleum (Beijing), Beijing 102249, China

(Corresponding Author: Email: ningzhengfu313@163.com)

ABSTRACT

Experiments on CO_2 displacement were conducted using cylindrical rock cores under various voltages, electric field modification times, and different injection-production parameters. The dynamic characteristics and contributing factors of direct current (DC) electric field-assisted CO_2 displacement on enhanced oil recovery were analyzed. The study shows that DC electric field-assisted CO_2 displacement development can be divided into four phases: high-speed oil and gas production induced by DC electric fields, oil-carrying gas production, DC electric-assisted dissolved gas drive, and low-speed oil production. Voltage and electric field modification time are the primary factors affecting the effectiveness of DC electric field-assisted CO_2 displacement development, followed by the CO_2 injection volume and extraction speed, with the CO_2 injection rate having the least impact. An optimal voltage exists that maximizes recovery efficiency; the longer the electric field modification time, the higher the recovery rate, although the rate of increase gradually slows. High volumes of CO_2 injection and slow extraction can enhance recovery rates. The stability of bottom-hole pressure in injection-production wells can serve as an indicator of the completion of electric field modification. The main contributors to the recovery rate in DC electric field-assisted CO_2 displacement development are the effects of the DC electric field on CO_2 dissolution and electroosmosis, followed by diffusion and CO_2 flow propagation.

Keywords: tight oil; DC electric field; CO_2 flooding; dynamic characteristics; oil displacement mechanism

1. INTRODUCTION

Efficient development of tight oil has long been a focal point in unconventional oil and gas exploration and production (LI L, 2021; HE Y, 2024; SYED F I, 2022; WANG Gaofeng, 2015). Tight oil is hosted in low-permeability reservoirs with gas-measured permeability less than 0.1×10^{-3} μm² under surface conditions (WANG Z, 2023; YUAN Zhou, 2021; ZHU Rukai, 2016). These reservoirs are characterized by poor physical properties and low resource abundance (JIA Chengzao, 2012). Depletion development strategies using volume fracturing techniques typically result in high initial production, rapid mid-term decline, and low overall recovery (CHEN Z, 2016; CHEN Z, 2022; HE Y, 2016; LIAO Guangzhi, 2022). Therefore, enhancing secondary and even tertiary oil recovery has become a critical issue for the efficient development of tight oil. As a high-intensity physical field, DC electric fields offer significant advantages in accelerating fluid flow and optimizing fluid properties (ZHANG W, 2020; WANG Z, 2024). DC-assisted CO_2 flooding not only improves recovery from tight reservoirs but also facilitates CO_2 geological sequestration, aligning with environmental sustainability goals and providing both theoretical foundation and technological support for their effective implementation (SHENG Y, 2023).

Conventional CO_2 flooding exhibits strongly nonlinear flow characteristics (WANG Z, 2023; XION Chunming, 2023), and the interactions between CO_2 and tight oil further complicate the flow behavior (HABIBI A, 2017; LIU Xiaolei, 2017). Researchers have demonstrated through laboratory experiments and numerical simulations that CO_2 flooding can improve the recovery of tight reservoirs to a certain extent (LI X, 2022; LI D, 2021; ZHOU X, 2019; REN B, 2015). Yu et al. (2021) identified CO_2 flooding as a key method for tight oil development, emphasizing that fractures are critical factors influencing recovery efficiency.

This study conducts laboratory experiments and numerical simulations of DC-assisted CO_2 flooding in tight oil reservoirs using large slab-shaped cores, cylindrical cores, and a self-developed high-temperature, high-pressure experimental system. Various development strategies and injection schemes are tested

This is a paper for the 11th Applied Energy Symposium: Low Carbon Cities & Urban Energy Systems (CUE2025), July 18-22, 2024, Kitakyushu, Japan.

to analyze the dynamic characteristics of CO_2 flooding under a direct current electric field, as well as the effects of key influencing factors on oil recovery.

2. EXPERIMENTAL DESIGN

2.1 Physical Simulation System for DC-Assisted CO_2 Flooding Using Slab-Shaped Cores

2.1.1 Physical Model Preparation

The physical model used in the experiment was constructed from a large outcrop rock core, with a permeability of 0.52×10^{-3} μm² and a porosity of 10.1%. The fabrication process of the physical model involved the following steps:

① A slab-shaped core measuring 25 cm in length and width and 3.5 cm in height was cut from the outcrop;

② Two boreholes were drilled diagonally to simulate vertical wellbores and enable pressure monitoring;

③ Along the boundary of the core, artificial fractures measuring 8 cm in length and 0.05 cm in width were created to simulate dynamic and hydraulic fractures. The hydraulic fractures were filled and compacted with crushed tight sandstone to ensure stable and limited conductivity, while the dynamic fractures were left unfilled to mimic extended fractures formed during long-term CO_2 flooding;

④ A single injection-production system and multiple pressure monitoring ports were installed on the surface of the model. Wells $1^{\#}$ and $2^{\#}$ served as the injection and production wells, respectively, while Wells $3^{\#}$ and $4^{\#}$ functioned as pressure monitoring points and were used for saturating the model with water and oil. Finally, the physical model was fully assembled and sealed.

2.1.2 High-Temperature and High-Pressure Experimental System

The high-temperature and high-pressure experimental system comprises several key components, including a temperature–pressure control system, a thermostatic chamber, pressure sensors, temperature sensors, displacement units, six-way valves, back-pressure valves, throttling valves, a DC power unit, gas–liquid separators, gas flow meters, a hand pump, an injection pump, a back-pressure pump, injection–production pipelines, and intermediate containers. Multiple displacement units were used to simulate the effects of varying electric field parameters and injection–production conditions on oil recovery. The positive and negative terminals of the DC power unit were connected to Wells $1^{\#}$ and $2^{\#}$ (or $2^{\#}$ and$1^{\#}$). To prevent the entire experimental setup from being energized, insulated sections were added to the injection–production pipelines around Wells $1^{\#}$ and $2^{\#}$, ensuring that current flowed only within the displacement units. The thermostatic chamber, in combination with the temperature–pressure control system and the hand pump, provided a high-temperature and high-pressure environment for the displacement experiments. Real-time monitoring of reservoir and bottomhole pressure was achieved through multiple pressure monitoring ports in the physical model connected to pressure sensors. The outlet flow rate was controlled using a throttling valve.

2.1.3 Experimental Design

Experimental Conditions: The experiments were conducted at a temperature of 40 °C and a confining pressure of 20 MPa.

Materials: The crude oil used in the experiments was tight oil maintained at 40 °C, with a viscosity of 8.5 mPa·s. The injection water was a 0.05 mol/L NaCl solution, with a viscosity of 0.653 mPa·s. The CO_2 gas used had a purity of 99.999%.

Experimental Scheme: Based on the experimental objectives, a total of 20 test scenarios were designed by varying the DC voltage, electric field treatment duration, CO_2 injection volume, production rate, and CO_2 injection rate.

Experimental Procedure:

① A 0.05 mol/L NaCl solution was injected into the slab-shaped core from port $4^{\#}$ at a constant flow rate of 0.1 mL/min until the injected volume reached 2 pore volumes (PV), and a stable water flow was observed at the outlet (port $3^{\#}$), indicating full water saturation of the core.

② Tight oil was then injected from port $4^{\#}$ at the same constant flow rate. Injection continued until the cumulative injected volume reached 3 PV and a continuous oil flow was observed at the outlet. The outlet was then closed, and oil injection continued until the inlet pressure increased to the preset formation pressure of 14 MPa, completing oil saturation of the core.

③ The saturated core was aged by static placement for 3 days.

④ A direct current was applied to the core by connecting the positive and negative terminals of the DC power supply to ports $1^{\#}$ and $2^{\#}$ (or $2^{\#}$ and$1^{\#}$). Pressure sensors at various monitoring points recorded real-time pressure responses during the electric field treatment.

⑤ The back-pressure valve at production well 2# was opened, and the outlet pressure was set to 6 MPa to conduct a depletion production stage. Production continued until no fluid was produced at port 3#.

⑥ CO_2 was injected from port 1# at a constant flow rate while keeping port 2# open, initiating the CO_2 flooding experiment under the assistance of a DC electric field. The outlet pressure was set to 3 MPa, and the produced fluid and gas volumes were recorded until a stable water flow was observed at the outlet.

⑦ Replace the core and repeat steps ① – ⑥ to complete all experimental scenarios.

2.2 DC-Assisted CO_2 Flooding in Cylindrical Cores

The cylindrical and slab-shaped cores were obtained from the same outcrop to ensure comparable physical properties. The cylindrical cores measured 2.5 cm in diameter and 5 cm in length. Oil recovery during CO_2 flooding was calculated using the mass balance method.

The experimental procedure was as follows:

① The cylindrical core was saturated with tight oil using a constant flow rate displacement until a continuous oil flow was observed at the outlet. Injection was then stopped to stabilize the core pressure at 9 MPa.

② In Experiments 22 and 23, CO_2 was injected for displacement, while in Experiments 24 and 25, tight oil was used as the displacing fluid. A direct current was applied across both ends of the core, and the outlet was closed. CO_2 or tight oil was injected at a constant flow rate until the internal core pressure reached the original formation pressure (14 MPa).

③ The injection end was then closed and the outlet was opened to perform pressure depletion production until no fluid was produced from the outlet.

④ After the experiment, the core was weighed to calculate oil recovery.

3. EXPERIMENTAL RESULTS AND ANALYSIS

3.1 Depletion Characteristics of Slab-Shaped Cores

In Experiment 1, the pressure of the slab-shaped core decreased from 14 MPa to 6 MPa, resulting in a recovery factor of 10.2%. The Arps decline curve model was used to fit the experimental data (Figure 1), showing a strong correlation between decline rate and production. The decline followed a hyperbolic trend with a decline exponent of 0.7942, which is close to values observed in field cases, indicating the reasonableness of the experimental design.

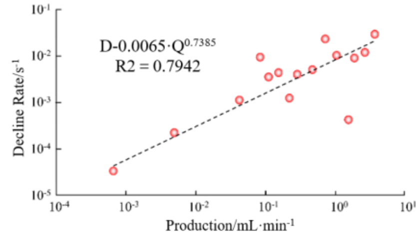

Fig. 1 Relationship Between Decline Rate and Production During Depletion Development in Slab-Shaped Cores

3.2 Production Characteristics of DC-Assisted CO_2 Displacement in Slab-Shaped Cores

The bottom-hole pressure, cumulative oil production, and cumulative gas production during CO_2 flooding with and without DC electric field assistance are shown in Figure 2. The application of a DC electric field accelerated the pressure drop at the early stage of production and increased cumulative oil and gas production by 20% to 53%.

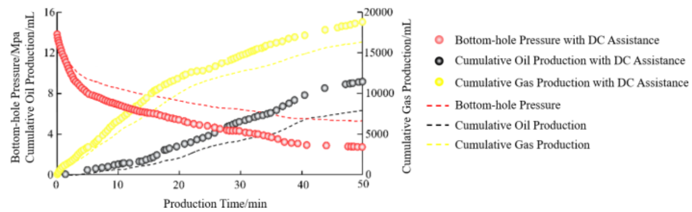

Fig. 2 Production Performance Curves During CO_2 Flooding with and without DC Electric Field Assistance

The relationships between bottom-hole pressure, oil production rate, and gas production rate over production time, with and without DC electric field assistance, are shown in Figure 3. Under DC-assisted CO_2 flooding, the dynamic production process can be divided into four stages:

① DC-induced high-rate oil production stage (0 – 10 min): Driven by the preferential flow paths induced by the electric field, a large amount of oil and a small amount of gas are produced rapidly, accompanied by a sharp drop in bottom-hole pressure.

② Gas-assisted oil production stage (20–30 min): Influenced by free CO_2 gas, oil swells with the gas in the preferential flow zones, and the sharp pressure drop at the bottom hole causes the free gas to expand and displace the oil.

③ DC-assisted solution gas drive stage (30–35 min): CO_2 transitions from free gas to dissolved gas. Due to the enhanced solubility of CO_2 in the electrically modified tight oil, the oil production rate increases significantly in a short period—though less than in Stage ①.

④ Low-rate oil production stage (35 – 50 min): As the effect of solution gas drive weakens, bottom-hole pressure continues to decline. Combined with the reduced liquid supply capacity of the core and a smaller production pressure differential, both oil and gas production rates gradually approach zero.

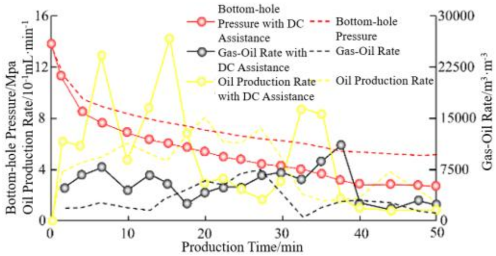

Fig. 3 Production Performance vs. Time Curves with and without DC Electric Field Assistance

The pressure responses corresponding to different stages of dynamic development after electrification are illustrated in Figure 4. Tight oil initially flows preferentially through the dominant flow zones induced by the DC electric field, accompanied by CO_2 displacement, forming the DC-induced high-rate oil production stage (Figure 4a). During the gas-assisted oil production stage, oil and gas are produced at relatively lower rates, while the displacement and pressure response propagate to the distal regions of the planar core model (Figure 4b). In the DC-assisted solution gas drive stage (Figure 4c), CO_2 rapidly dissolves into the tight oil; as bottom-hole pressure decreases, CO_2 comes out of solution and expands, resulting in relatively high oil production. As the reservoir pressure within the planar core model approaches the outlet pressure, the solution gas drive effect diminishes, marking the transition into the low-rate oil production stage.

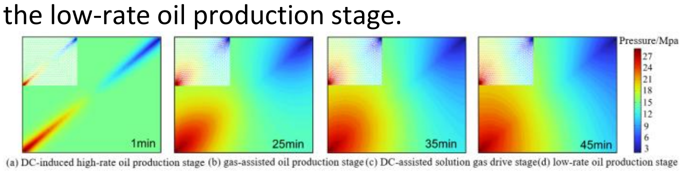

Fig. 4 Pressure Response at Different Production Stages After Electrification

As shown in Figure 5, the oil recovery factor as a function of bottom-hole pressure exhibits a similar trend for both DC-assisted CO_2 flooding and conventional CO_2 flooding. In both cases, the recovery factor increases slowly during the early stage of production and accelerates in the later stage. When the bottom-hole pressure reaches 3 MPa, the application of a direct current electric field improves the recovery factor by 14.5%. A significant increase in recovery is observed once the pressure drops to 12.9 MPa under DC-assisted conditions, whereas conventional CO_2 flooding requires the pressure to drop to 10.7 MPa to achieve a comparable improvement.

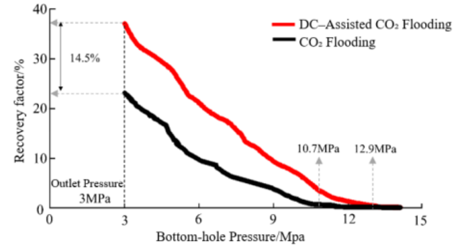

Fig. 5 Recovery Factor vs. Bottom-Hole Pressure Curve

The CO_2 volumetric expansion factor as the core model pressure decreases from the original reservoir pressure (14 MPa) to the outlet pressure (3 MPa) is shown in Figure 6. The volumetric expansion factor of CO_2 is defined by Equation (1):

$$E = \frac{V_i}{V_0} = \frac{\rho_0}{\rho_i} \qquad (1)$$

In the equation, E is the CO_2 volumetric expansion factor; V_i is the expanded volume of CO_2, in cubic meters (m^3); V_0 is the initial volume of CO_2 under original conditions, in cubic meters (m^3); ρ_i is the density of CO_2 at the expanded state, in kilograms per cubic meter (kg/m^3); and ρ_0 is the density of CO_2 under initial conditions, in kilograms per cubic meter (kg/m^3).

The turning point of the CO_2 volumetric expansion factor occurs at pressures of 13 MPa and 11 MPa under the DC electric field-assisted CO_2 flooding and conventional CO_2 flooding methods, respectively (see Figure 6), which is consistent with the turning points of the recovery factor shown in Figure 5. Meanwhile, the DC electric field increases the CO_2 volumetric expansion factor by 2.3 times, indicating that the CO_2 expansion effect is a significant driving force in CO_2 flooding development. The DC electric field can enhance the CO_2 expansion effect, thereby improving the recovery factor.

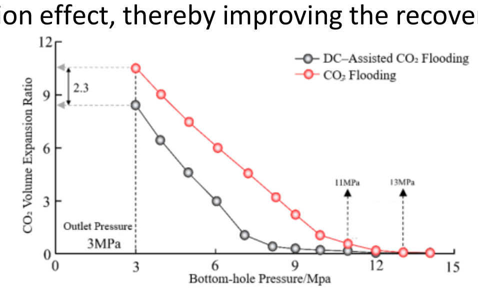

Fig. 6 Relationship Between CO_2 Volume Expansion Ratio and Bottom-Hole Pressure

3.3 Influencing Factors of Electric Field-Assisted CO_2 Flooding

3.3.1 Direct Current Voltage

The experimental data obtained from experiments 1 to 5 are shown in Figure 7. With the increase of voltage, the recovery factor exhibits a trend of first rising and then declining, reaching a maximum at 8 V. Based on the trend line prediction, the recovery factor is estimated to be 28% at 2 V, which is consistent with the experimental value of 27.2%. The results indicate that at low voltages, the recovery factor is positively correlated with voltage, while at high voltages, the correlation is negative. An optimal voltage exists at which the recovery factor reaches its peak.

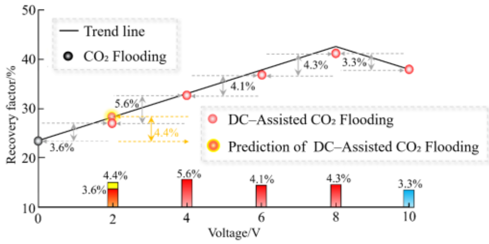

Fig. 7 Recovery Factor vs. Voltage Curve

3.3.2 Direct Current Treatment Time

The experimental data from experiments 1 and 6 to 9 are shown in Figure 8. As the duration of the electric field modification increases, the recovery factor improves, but the rate of improvement gradually decreases. Meanwhile, when the electric field modification time exceeds 8.8 hours, the bottom-hole pressures of the injection and production wells gradually stabilize. The effective influence range of DC-induced viscosity reduction and electroosmotic flow also reaches a steady state, indicating that prolonged electric field modification contributes less to recovery. Whether the bottom-hole pressures of the injection and production wells have stabilized can serve as a criterion for judging the completion of electric field modification. The more wells with stable bottom-hole pressures, the more thoroughly the reservoir within the well pattern has been modified.

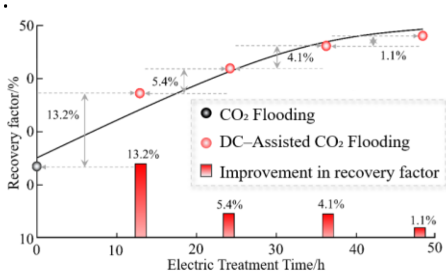

Fig. 8 Recovery Factor vs. Electric Treatment Time Curve

3.3.3 CO_2 Injection Volume

CO_2 injection volume significantly influences the effectiveness of CO_2 flooding development. Experimental data (Experiments 10–13) on CO_2 injection volume, recovery factor, and gas-oil displacement ratio are shown in Figure 9. As the CO_2 injection volume increased from 5.64 g to 15.71 g, the CO_2 flooding recovery factor increased by 11%, while the gas-oil displacement ratio decreased by 0.25 g·g^{-1}. Under the assistance of the DC electric field, the CO_2 flooding recovery factor improved by 14.4%, and the gas-oil displacement ratio decreased by 0.11 g·g^{-1}. It is noteworthy that the DC electric field significantly enhances both the CO_2 flooding recovery factor and the gas-oil displacement ratio, but an optimal value exists. At low CO_2 injection volumes, the increase in recovery factor and gas-oil displacement ratio due to the DC electric field is more pronounced; but, at higher CO_2 injection volumes, the improvement rate slows down.

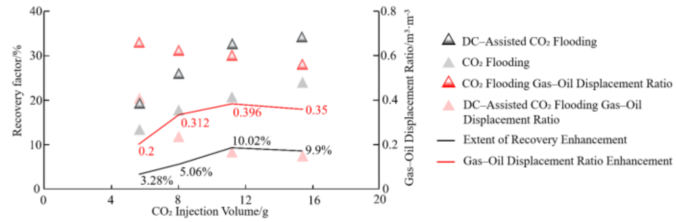

Fig. 9 Curves of Recovery Factor and Gas–Oil Displacement Ratio vs. CO_2 Injection Volume

3.3.4 Production Time

Experimental data (Experiments 1 and 14–17) are shown in Figure 10. As the opening degree of the throttling valve increases, the CO_2 flooding development time is extended. Lowering the production rate expands the effective influence range of the DC electric field electroosmosis, resulting in an increase in recovery factor from 25.2% to 42.9%, a rise of 17.7%. Compared with Experiment 1, when the throttling valve opening reaches 60%, the DC electric field enhances the recovery factor by 14.5%. Overall, reducing the production rate benefits the improvement of recovery factor in DC electric field-assisted CO_2 flooding development.

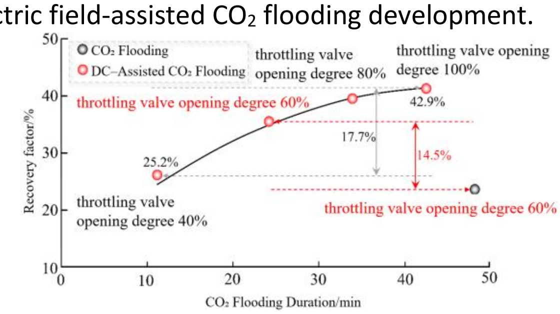

Fig. 10 Recovery Factor vs. Production Time Curve

4. CONCLUSIONS

The development of CO_2 flooding assisted by a DC electric field can be divided into four stages: DC-induced high-speed oil production, gas production carrying oil, DC-assisted dissolved gas drive, and low-speed oil production.

Voltage and the duration of electric field treatment are the main factors influencing the effectiveness of DC electric field-assisted CO_2 flooding, followed by CO_2 injection volume and production rate. Among these, the

CO_2 injection rate has the least impact on development results. There exists an optimal voltage that maximizes recovery; the longer the electric field treatment time, the greater the recovery, although the rate of increase gradually slows down. As the CO_2 injection volume increases and the production rate decreases, the recovery factor gradually improves. Whether the bottom-hole pressure of the injection and production wells remains stable can serve as an indicator of the completion of electric field treatment. The optimal voltage, CO_2 injection volume, and production rate need to be calculated according to the actual conditions of the reservoir.

The enhanced recovery from DC electric field-assisted CO_2 flooding mainly comes from DC-assisted CO_2 dissolution sweep and electro-osmotic sweep, followed by diffusion sweep and CO_2 flow sweep.

ACKNOWLEDGEMENT

This work was supported by Science Foundation of China University of Petroleum ， Beijing (No.2462025XKBH025) and the Postdoctoral Fellowship Program (Grade B) of China Postdoctoral Science Foundation under Grant Number GZB20250681.

REFERENCE

[1] LI L, CHEN Z, SU Y-L, et al. Experimental Investigation on enhanced-oil-recovery mechanisms of using supercritical carbon dioxide as prefracturing energized fluid in tight oil reservoir[J]. SPE Journal, 2021, 26(05): 3300-15.

[2] HE Y, SHANG Y, WU W, et al. Investigating recovery potential through depletion development of tight oil reservoirs via NMR technology[J]. Energy & Fuels, 2024, 38(1): 333-40.

[3] SYED F I, MUTHER T, VAN V P, et al. Numerical trend analysis for factors affecting EOR performance and CO_2 storage in tight oil reservoirs[J]. Fuel, 2022, 316: 123370.

[4] WANG Gaofeng, ZHENG Xiongjie, ZHANG Yu, et al. A new screening method of low permeability reservoirs suitable for CO_2 flooding[J]. Petroleum Exploration and Development, 2015, 42(3): 390-6.

[5] WANG Z, NING Z, ZHAN J, et al. Evaluation of effects of waterflooding-induced bilayer fractures on tight reservoir using pressure-transient analysis method[J]. SPE Reservoir Evaluation & Engineering, 2023, 26(04): 1378-401.

[6] YUAN Zhou, LIAO Xinwei, ZHANG Kuaile, et al. The effect of inorganic salt precipitation on oil recovery during CO_2 flooding: A case study of Chang 8 block in Changqing oilfield, NW China[J]. Petroleum Exploration and Development, 2021, 48(2): 442-9.

[7] ZHU Rukai, WU Songtao, SU Ling, et al. Problems and future works of porous texture characterization of tight reservoirs in China[J]. Acta Petrolei Sinica, 2016, 37(11): 1323-36.

[8] JIA Chengzao, ZOU Caineng, LI Jianzhong, et al. Assessment criteria, main types, basic features and resource prospects of the tight oil in China [J]. Acta Petrolei Sinica, 2012, 33(3): 343-50.

[9] CHEN Z, LIAO X, ZHAO X, et al. A semianalytical approach for obtaining type curves of multiple-fractured horizontal wells with secondary-fracture networks[J]. SPE Journal, 2016, 21(02): 538-49.

[10] CHEN Z, LIAO X. A workflow of fracture geometry diagnostics of unconventional wells with complex fracture networks coupling fracture mapping and well testing[J]. Journal of Petroleum Science and Engineering, 2022, 208: 109310.

[11] HE Y, CHENG S, LI S, et al. A semianalytical methodology to diagnose the locations of underperforming hydraulic fractures through pressure-transient analysis in tight gas reservoir[J]. SPE Journal, 2016, 22(03): 924-39.

[12] LIAO Guangzhi, HE Dongbo, WANG Gaofeng, et al. Discussion on the limit recovery factor of carbon dioxide flooding in a permanent sequestration scenario[J]. Petroleum Exploration and Development, 2022, 49(6): 1463-70.

[13] ZHANG W, NING Z, CHENG Z, et al. Experimental investigation of the role of DC voltage in the wettability alteration in tight sandstones[J]. Langmuir, 2020, 36(40): 11985-95.

[14] WANG Z, NING Z, GUO W, et al. DC electric field assisted heat extraction evaluation via water circulation in abandoned production well patterns: semi-analytical and numerical models[J]. Renewable Energy, 2024, 228: 120663.

[15] SHENG Y, CAO Y. The promotion mechanism of digital platformization of enterprises for “double carbon” goal: a Chinese case study [J]. Environmental Science and Pollution Research, 2023, 30(33): 80741-57.

[16] WANG Z, NING Z, GUO W, et al. Monitoring dynamic rock fracture behavior after long-term CO_2 injection in tight reservoir: semi-analytical model and case study[J]. Energy & Fuels, 2023, 37(23): 18928-44.

[17] XION Chunming, WEI Falin, YANG Haiyang, et al. Characteristics and mechanism of smart fluid for sweeping control during CO2 flooding[J]. Petroleum Exploration and Development, 2023, 50(3): 648-56.

[18] HABIBI A, YASSIN M R, DEHGHANPOUR H, et al. Experimental investigation of CO_2-oil interactions in tight rocks: a montney case study[J]. Fuel, 2017, 203: 853-67.

[19] LIU Xiaolei, QIN Jishun, HAN Haishui, et al. Multiphase boundary of C16+ heavy n-alkanes and CO_2 systems[J]. Petroleum Exploration and Development, 2017, 44(1): 105-10.

[20] LI X, XUE J, WANG Y, et al. Experimental study of oil recovery from pore of different sizes in tight sandstone reservoirs during CO_2 flooding[J]. Journal of Petroleum Science and Engineering, 2022, 208: 109740.

[21] LI D, SARAJI S, JIAO Z, et al. CO_2 injection strategies for enhanced oil recovery and geological sequestration in a tight reservoir: an experimental study[J]. Fuel, 2021, 284: 119013.

[22] ZHOU X, YUAN Q, ZHANG Y, et al. Performance evaluation of CO_2 flooding process in tight oil reservoir via experimental and numerical simulation studies[J]. Fuel, 2019, 236: 730-46.

[23] REN B, ZHANG L, HUANG H, et al. Performance evaluation and mechanisms study of near-miscible CO_2 flooding in a tight oil reservoir of Jilin Oilfield China[J]. Journal of Natural Gas Science and Engineering, 2015, 27: 1796-805.